

# Haemodynamic stress-induced breaches of the arterial intima trigger inflammation and drive atherogenesis

Grégory Franck<sup>1</sup>, Guillaume Even<sup>1</sup>, Alexandre Gautier<sup>1</sup>, Manuel Salinas<sup>2</sup>, Alexia Loste<sup>1</sup>, Emanuele Procopio<sup>1</sup>, Anh-Thu Gaston<sup>1</sup>, Marion Morvan<sup>1</sup>, Sébastien Dupont<sup>1</sup>, Catherine Deschildre<sup>1</sup>, Sophie Berissi<sup>3</sup>, Jamila Laschet<sup>1</sup>, Patrick Nataf<sup>4</sup>, Antonino Nicoletti<sup>1</sup>, Jean-Baptiste Michel<sup>1</sup>, and Giuseppina Caligiuri<sup>1,5\*</sup>

<sup>1</sup>INSERM U1148, Laboratory for Vascular Translational Science (LVTS), DHU FIRE, University Paris Diderot, Sorbonne Paris Cité, 46 rue Henri Huchard, 75018 Paris, France;

<sup>2</sup>Department of Engineering and Technology, College of Engineering and Computing, Nova Southeastern University, 3301 College Avenue, Fort Lauderdale, FL, USA;

<sup>3</sup>Histomorphology platform, SFR Necker INSERM (INSERM US24-CNRS UMS3633), 24, bd du Montparnasse 75015 Paris, France; <sup>4</sup>Department of Cardiac Surgery, University Hospital Xavier Bichat, AP-HP, 46 rue Henri Huchard, 75018 Paris, France; and <sup>5</sup>Department of Cardiology, University Hospital Xavier Bichat, AP-HP, 46 rue Henri Huchard, 75018 Paris, France

Received 24 September 2018; revised 18 October 2018; editorial decision 14 November 2018; accepted 15 November 2018

## Aims

Inflammatory mediators, including blood cells and their products, contribute critically to atherogenesis, but the igniting triggers of inflammation remain elusive. Atherosclerosis develops at sites of flow perturbation, where the enhanced haemodynamic stress could initiate the atherogenic inflammatory process due to the occurrence of mechanic injury. We investigated the role of haemodynamic stress-induced breaches, allowing the entry of blood cells in the arterial intima, in triggering inflammation-driven atherogenesis.

## Methods and results

Human coronary samples isolated from explanted hearts, ( $n = 47$ ) displayed signs of blood entry (detected by the presence of iron, ferritin, and glycophorin A) in the subintimal space (54%) as assessed by histology, immunofluorescence, high resolution episcopic microscopy, and scanning electron microscopy. Computational flow dynamic analysis showed that intimal haemorrhagic events occurred at sites of flow disturbance. Experimental carotid arteries from *Apoe* deficient mice showed discrete endothelial breaches and intimal haemorrhagic events specifically occurring at the site of flow perturbation, within 3 days after the exacerbation of the local haemodynamic stress. Endothelial tearing was associated with increased VCAM-1 expression and, within 7 days, substantial Ly6G<sup>+</sup> leucocytes accumulated at the sites of erythrocyte-derived iron and lipids droplets accumulation, pathological intimal thickening and positive oil red O staining. The formation of fatty streaks at the sites of intimal breaches was prevented by the depletion of Ly6G<sup>+</sup> leucocytes, suggesting that the local injury driven by haemodynamic stress-induced breaches triggers atherogenic inflammation.

## Conclusion

Haemodynamic-driven breaches of the arterial intima drive atherogenic inflammation by triggering the recruitment of leucocyte at sites of disturbed arterial flow.

## Keywords

Endothelial cells • Flow disturbance • Atherogenesis • Breaches

\* Corresponding author. Tel: +33 1 40257556, Fax: +33 1 40258602, Email: giuseppina.caligiuri@inserm.fr

Published on behalf of the European Society of Cardiology. All rights reserved. © The Author(s) 2018. For permissions, please email: journals.permissions@oup.com.

## Translational perspective

By revisiting the earliest events occurring at the atherogenic sites in human coronary arteries and by demonstrating that mechanic wounding can be the *primum movens* of inflammation at these sites, our study may drive a paradigm shift of plaque formation towards biomechanics considerations. Future treatments aimed at preventing plaque development might therefore have to deal with the haemodynamic stress-induced breaches and/or their consequences on the biology of arteries. Of note, wall haemoglobin iron imaging could also redefine early health assessment of our arteries, partly through a better detection of subclinical atherosclerosis. This latter approach, yet, will have to rely on better spatial imaging depth and resolution.

## Introduction

The leakage of erythrocytes from intraplaque neovessels is known to contribute to atherosclerotic plaque progression, but erythrocyte accumulation in the subintimal space at sites of flow perturbation may also participate in the initiation of atherogenesis, as suggested by a recent work from our laboratory.<sup>1</sup> Yet, the mechanisms linking flow perturbation, erythrocytes entry in the subintimal space, and atherogenesis are not known.

The impact of flow perturbation on endothelial cell (EC) dysfunction, associated with atherogenesis, has undergone extensive study. The physiologic barrier and tone-regulation functions of ECs give way to pro-inflammatory and pro-fibrotic properties within arterial segments displaying complex geometries (bifurcations, stenosis, and dilation), sites prone to develop atherosclerosis.<sup>2</sup> Endothelial disruption on established plaques may result from EC death by apoptosis or anoikis and detachment from the basement membrane.<sup>3</sup>

The physical damage of the endothelial barrier, possibly induced by the particularly high haemodynamic stress in the arterial circulation, has instead received much less attention. Pioneering work in the 80s had reported the presence of numerous local intimal lesions, designated 'endothelial breaches', characterized by the presence of focal EC desquamation in association with the accumulation of formed elements of blood in the subintimal space, at sites of perturbed flow of human coronary arteries.<sup>4</sup> Extensive focus on mechanisms of EC dysfunction that involve LDL-triggered inflammation tended to supersede these earlier observations.

In line with our recent work and with these previous observations, we hypothesized that mechanically-induced endothelial breaches can indeed influence the site of atherosclerotic lesion formation by triggering the local inflammatory process that results from the regional accumulation of erythrocyte-derived lipids and iron in the arterial intima.

Here, we studied the position and functional significance of endothelial breaches present in non-atherosclerotic human coronary arteries by histomorphometrical and ultrastructural analysis, to link flow perturbation with anatomic findings. We also provide an *in vivo* proof of concept by using an experimental approach aimed at exacerbating the haemodynamic stress in arterial segments prone to atherosclerosis in mice, paving the way for further mechanistic studies.

## Methods

Human hearts freshly explanted from cardiac transplant recipients were obtained according to protocols approved by the INSERM ethic

committee. The explants were flushed with saline and the main coronary arteries were immediately isolated under a surgical microscope by an experienced researcher. Apolipoprotein E (*apoe*<sup>-/-</sup>) deficient male C57BL/6 mice (in-house breeding), 25–30 g, were used in conditions approved by the INSERM ethic committee. Animals were submitted to carotid artery constriction using a custom device as previously described<sup>5</sup> and subjected to continuous perfusion of Angiotensin (Ang) II, delivered by osmotic pumps implanted subcutaneously. Quantitative data are expressed as mean  $\pm$  standard deviation and comparisons were evaluated using Prism<sup>®</sup> (GraphPad) and non-parametric tests. Differences were considered statistically significant when the  $P < 0.05$  level (unadjusted  $P$ -values).

Please see [Supplementary material online](#) for detailed description of the methods.

## Results

### Endothelial breaches in human coronary arteries

Blood accumulation was observed from the intimal side of longitudinally opened coronary arteries isolated from explanted hearts (*Figure 1A*). To assess the extent of this observation, we used the Perls + diaminobenzidine (DAB) staining to specifically detect the iron deriving from red blood cells (negative control shown in [Supplementary material online, Figure S1A](#)), as previously described.<sup>6</sup> In 17/31 (54.8%) of the analysed samples, Perls + DAB staining revealed that erythrocytes with haemoglobin-derived iron localized superficially, in the most superficial layer of the intima in contact with lumen (*Figure 1B*). Glycophorin A (GpA), a membrane bound receptor specifically expressed by erythrocytes and ferritin, an iron storage molecule increasingly expressed in the presence of iron, affirmed independently the presence of erythrocytes in the superficial intima (*Figure 1C*). Serial longitudinal sections showed that, in these subintimal areas, iron consistently colocalized with Oil red O positive lipids (*Figure 1D*) comprised in ceroids and cholesterol crystals ([Supplementary material online, Figure S2](#)). High resolution episcopic microscopy (HREM) performed on coronary samples ( $n = 3$ ) revealed the presence of iron in two distinct vessel wall compartments (*Figure 1E* and [Supplementary material online, Figure S1B](#)): deep within the atheromatous plaque ('intra-plaque'), and superficial in intimal areas ('Luminal'). Of note, iron detected in the subintimal space did not contact the outer arterial wall layers, suggesting that the source of erythrocytes furnishing intimal iron does not derive from the adventitial microvessels but rather from the luminal macrocirculation

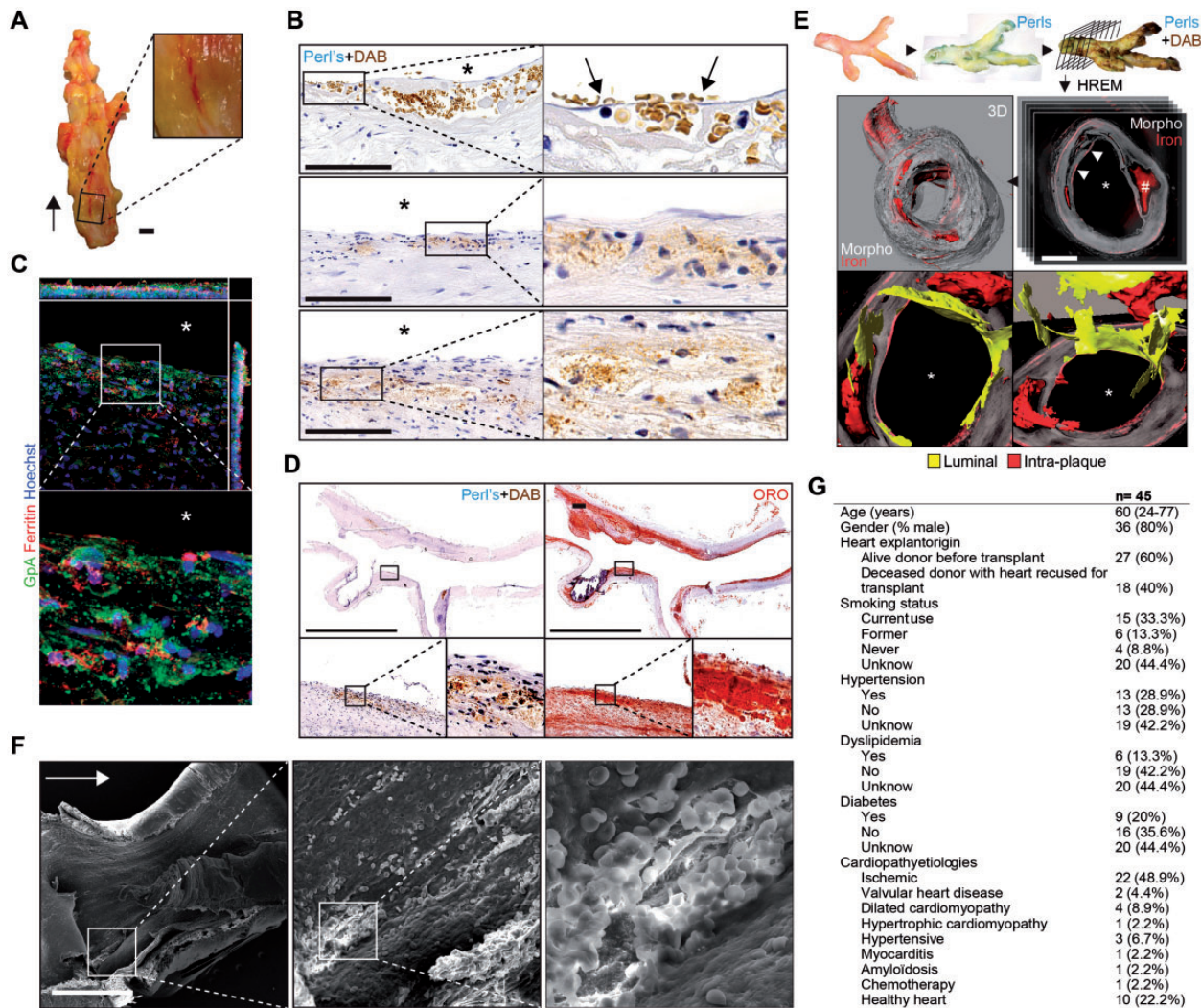


**Figure 1** Endothelial breaches in the intima of human coronary arteries. (A) Freshly explanted coronary artery exposed for *en face* intima visualization. Arrow shows flow orientation. Scale bar: 1 mm. (B) Erythrocyte and erythrocyte-derived iron accumulation in the superficial intima of human coronary arteries as shown with a Perl's + diaminobenzidine (DAB) staining. Scale bar: 100  $\mu$ m. (C) Glycophorin A (GpA, green) and ferritin (red) staining showing red blood cell accumulation in the intima of a coronary section. Star shows the lumen. (D) Serial sections of a coronary artery with early atheromatous lesions, stained with Perl's + DAB (iron) and Oil red O (ORO, lipids). Scale bar: 1 cm. (E) High resolution episcopic microscopy performed on a coronary artery sample stained with Perl's + DAB, delineating luminal and intra-plaque iron signal. Star shows the lumen. Arrowhead shows luminal iron signal; Ash points at deeper intra-plaque iron deposits. Scale bar: 2 mm. (F) Explanted coronary arteries without signs of atherosclerosis visualized *en face* by scanning electron microscopy. Scale bar: 500  $\mu$ m. Arrow: flow orientation. (G) Clinical characteristic of donors from which the coronary arteries were prepared.

(Supplementary material online, Video). Small and superficial endothelial breaches, tangential to the flow orientation and engulfing numerous erythrocytes, were consistently observed in human coronary arteries analysed *en face* by scanning electron microscopy (SEM,  $n=3$ , Figure 1F). The clinical characteristics of the patients from whom all the specimens were harvested are reported in Figure 1G; of note, 22.2% of analysed hearts were non-atherosclerotic, and artery segments with macroscopic advanced atherosclerosis and/or macroscopic haemorrhages ( $n=18$ ,

Supplementary material online, Figure S3) were excluded for the evaluation of endothelial breaches. These findings therefore suggest that endothelial breaches, characterized by the presence of erythrocytes and erythrocyte-derived iron accumulation in continuity with the arterial lumen, constitute an initial vessel insult at sites prone to atherosclerotic lesions formation. In addition, the 'luminal' areas of iron accumulation were not evenly distributed but clustered, indicating that local conditions, likely haemorrhological, could determine where the endothelial breaches can occur.

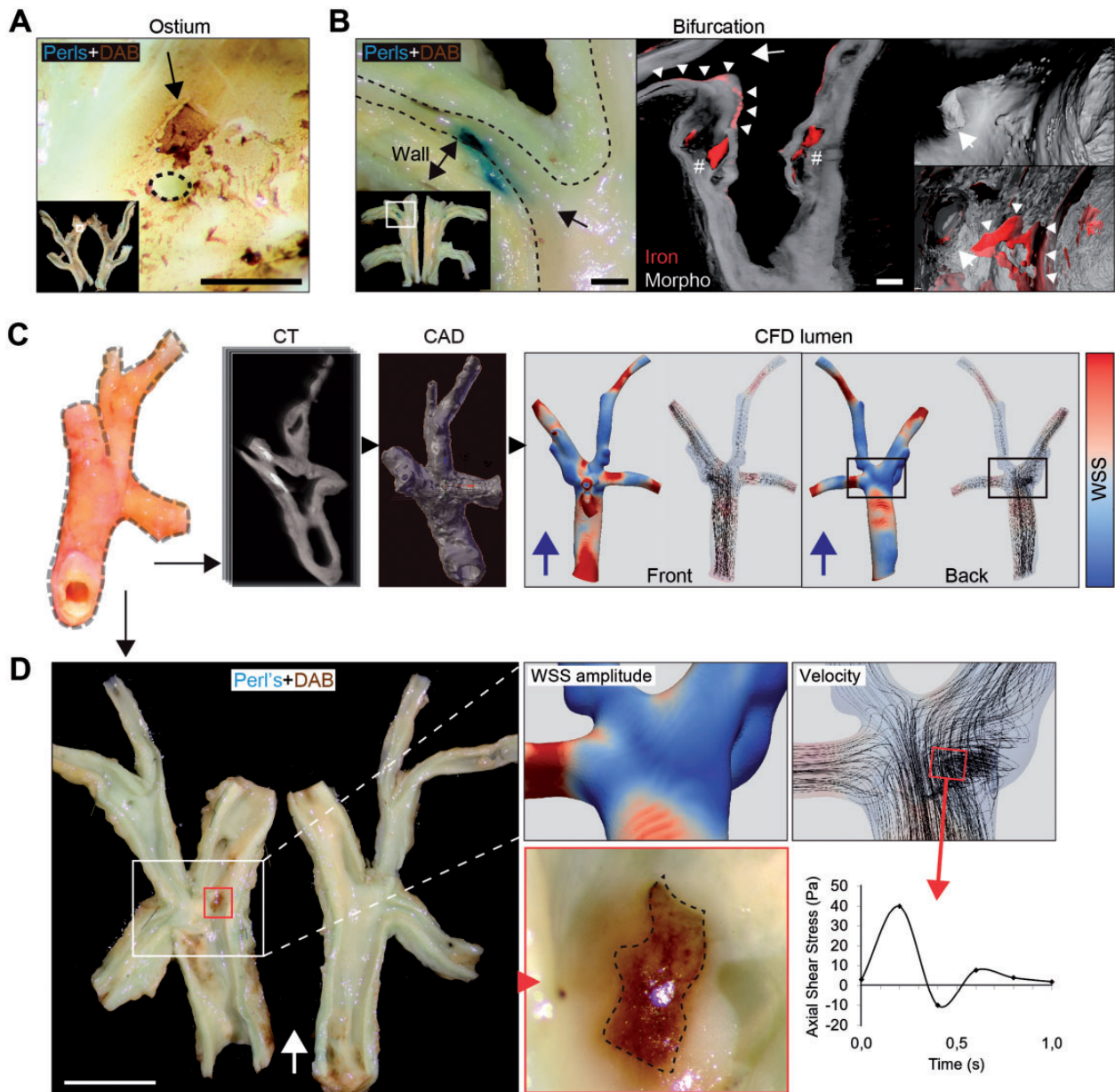


**Figure 2** Impact of arterial geometry and haemodynamic on intimal breaches and iron deposits. (A) Localization of Perl's + DAB positive areas near an ostium in a human coronary artery. Scale bar: 1 mm. (B) Perl's + DAB-positive staining in the superficial intima within a bifurcation (left). High resolution episcopic microscopy showing the presence of iron deposits in superficial intima (right, arrowheads). Hashes point at deeper intra-plaque iron deposits. Arrow indicates the bifurcation. Scale bar: 1 mm. (C and D) Dual analysis of human coronary artery samples: first by computational flow dynamics after reconstitution by computed tomography scan imaging and computer-aided design (C), second by labelling of wall iron with a Perl's + DAB staining on the whole mount preparation of the same coronary artery (D). For computational flow dynamics, wall shear stress amplitude and flow velocity vectors are graphically represented. Arrows show flow orientation. Dashed lines delineate superficial iron deposits (intimal breach). Scale bar: 1 cm. CAD, computer-aided design; CFD, computational flow dynamics; CT, computed tomography; WSS, wall shear stress.

### Arterial geometry-based flow pattern at the site of intimal breaches

Wall iron detection in coronary arteries using the Perl's + DAB staining of whole mount preparations revealed the presence of intimal

haemorrhages mainly near ostia (Figure 2A) and bifurcations (Figure 2B). As complex vascular geometries associate with flow disturbances,<sup>7</sup> specific haemodynamic may influence the presence of intimal breaches. To address this issue, a computational flow dynamic

study was performed on high resolution computed tomography (CT) scans of Perl's + DAB stained coronary whole artery samples ( $n = 10$ ). Lumen reconstitution and geometry analysis-based simulation of the flow pattern (Figure 2C) showed the presence of disturbed flow velocity vectors and oscillatory axial stress in areas exhibiting iron deposits due to intimal breaches (Figure 2D). These observations strongly suggest that the formation of the observed intimal breaches is linked to the enhanced haemodynamic-stress exerted by the flow perturbations occurring at sites of complex arterial geometry. Evaluation of this hypothesis used an *in vivo* strategy aimed at recapitulating enhanced local haemodynamic stress and its putative link with the occurrence of experimental intimal breaches and the formation of fatty streaks at these sites, due to the ensuing inflammatory process, in atherosclerosis-prone mice.

### Enhanced local haemodynamic stress drives the formation of intimal breaches, erythrocyte accumulation, inflammation and fatty streak formation *in vivo*

To probe how haemodynamic perturbations promote vascular damage, we have evaluated the impact of flow perturbation due to complex arterial geometry combined with increased blood pressure on the morphology of the left common carotid artery in *apoe*<sup>-/-</sup> mice subjected to a perivascular cuff to induce partial stenosis ( $n = 3$  per group, Figure 3A) and continuous Ang II perfusion. These experimental conditions generate specific flow perturbations in the carotid segment downstream the constrictive cuff (CC), as assessed by intravital imaging using a systemic injection of a tracer dye and computational cardiac cycle-gated flow dynamics (Supplementary material online, Figure S4). The downstream segment was not altered at Day 1 but the persistence of enhanced local flow perturbation for 3 days led to the formation of severe intimal associated with local erythrocyte accumulation at the site of perturbed flow, as assessed by the presence of both glycophorin A and ferritin (Figure 3B). The evaluation of consecutive sections from samples collected at different time points revealed that the occurrence of intimal damage was linked to the appearance of subintimal haemorrhages, increased expression of VCAM-1 by the involved luminal endothelium, and the accumulation of Ly6G<sup>+</sup> neutrophils at the sites of endothelial breaches. After 7 days, the vessel wall displayed partially healed features as underlined by almost complete endothelial coverage, but oil red O positive material, reflecting the formation of fatty streaks, coincided with the presence of granulocytes infiltrated in the subendothelial layer (Figure 3C). Interestingly, VCAM-1 expression increased over time and was proportional to the thickening of the injured intima (Figure 3D and Supplementary material online, Figure S5). *En face* analysis by SEM, in parallel sets of experiments terminated at Day 3, showed that the arterial segments located upstream the cuff or within the cuff, where the flow remains mostly laminar, exhibited an intact endothelium over the surface. In contrast, segments located downstream the cuff, within the site of flow perturbation, showed severe luminal defects, including intimal breaches oriented in the direction of flow, and EC desquamation. Local endothelial disruption was associated systematically with the accumulation of erythrocytes and leucocytes, presumably neutrophils (Figure 3F). Of note, neither the contralateral carotid without CC, nor the arterial segments upstream

or within the CC displayed comparable features (Supplementary material online, Figure S4). Control experiments used a sham procedure (no cuff) or the placement of a non-CC. We previously showed that none of these control conditions induced intimal defects.<sup>5</sup> Thus, the intimal breaches at sites of disturbed flow did not result from experimental artefacts, but rather from the experimental arterial haemodynamic stress.

### Intimal breaches associate with leucocyte infiltration in human samples

A rich neutrophil infiltrate was also present at the site of subintimal haemorrhage and intimal breaches in human coronary arteries, as detected by the detection of CD66b<sup>+</sup> granulocytes (the equivalent of murine Ly6G<sup>+</sup> leucocytes) (Figure 4A and B). *En face* and Z-stack analysis of whole mount preparations of arteries stained for ECs (CD31<sup>+</sup>) and myeloperoxidase (MPO)<sup>+</sup> cells confirmed the presence of granulocytes near the superficial intima (Figure 4C). The degree of local CD66b<sup>+</sup> cell count inversely correlated with the extent of endothelial continuity ( $P < 0.0001$ , Figure 4D and E). Testing whether the recruitment of neutrophils participates in the putative atherogenic inflammatory process at the sites of endothelial breaches used experiments aimed at preventing the function of Ly6G<sup>+</sup> leucocytes in mouse arteries submitted to our model of experimental haemodynamic stress exacerbation.

### Neutrophils recruitment is necessary for the atherogenic role played by the intimal breaches

Mice were injected with depleting doses of an antibody directed against both Ly6G (expressed by murine neutrophils) and Ly6C (expressed by both neutrophils and monocytes), or an isotype, twice (1 day before and again 1 day after the placement of the CC and the implantation of the Ang II osmotic pump, Figure 5A) to 8 to 10-week-old mice ( $n = 7$  per group). The administration of anti-Ly6C/G had no significant effect, when compared with the isotype group, on the values of systolic arterial pressure, which increased by 20% ( $P < 0.001$ ) by Day 3 (Figure 5B). Neutrophils as well as Ly6C<sup>high</sup> monocytes were effectively and selectively depleted as demonstrated by flow cytometry analysis of mouse peripheral blood leucocytes (Figure 5C and D, Supplementary material online, Figure S6). Neutrophil depletion prevented the appearance of intimal thickening of the carotid arteries exposed to flow perturbation (Figure 5E) in contrast with those of the isotype-treated group which showed severe intimal lesions characterized by erythrocyte and neutrophil infiltration. In-depth analysis of the luminal endothelium continuity revealed that, although to a lower extent, the endothelial integrity was disrupted also in the neutropenic mice (Figure 5F). *En face* analysis by SEM, in parallel sets of experiments ( $n = 3$ /group, Figure 5G), showed the presence of numerous leucocytes at the sites of intimal breaches, downstream the CC in the control group ('Isotype'), whereas carotids harvested from neutropenic mice displayed considerable signs of focal EC damage, with signs of detachment and blebbing, but almost no leucocytes *in situ* ('Anti-Ly6C/G'). Artefacts due to fixation and dehydration were excluded since exclusively healthy ECs were detectable in the control cuff segments, subjected to laminar flow pattern and high shear stress.

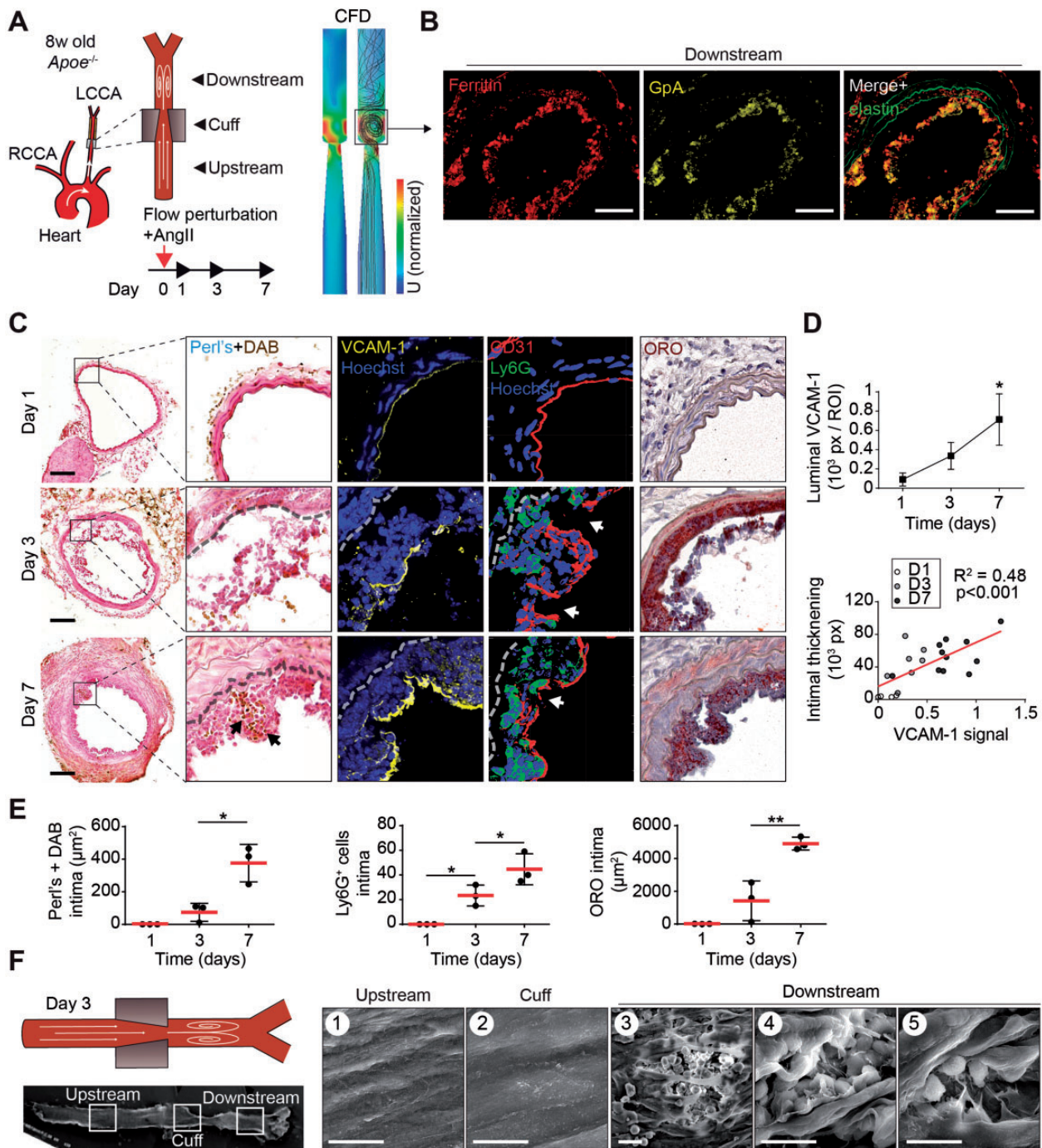


**Figure 3** *In vivo* model of haemodynamic stress-induced intimal breaches. (A) Generation of flow perturbation in the left common carotid artery of chow-fed *apoe*<sup>-/-</sup> mice, implanted with osmotic pumps delivering 1 mg Ang II/kg/day, by the application of a progressive constrictive cuff. LCCA, left common carotid artery; RCCA, right common carotid artery. Computational flow dynamics (CFD) showing flow perturbation downstream the cuff. (B) Immunostaining for ferritin (red) and glycophorin A (GpA, yellow) of left common carotid artery, downstream of flow perturbations for 3 days. Elastin (green, autofluorescence). (C) Kinetics of intimal breach formation at the site of flow perturbation after 1, 3, and 7 days. Perl's + DAB staining of iron deposits in the vessel wall (the squares indicate the localization of the details shown in the insets), immunofluorescent staining of VCAM-1 CD31 + Ly6G and Oil red O (ORO). Nuclei were stained with Hoechst 33342. White arrows show the location of endothelial breaches. Dashed line delimitates the internal elastic lamina. Scale bar: 100  $\mu$ m. (D) Quantification of the luminal VCAM-1 signal and regression analysis of luminal VCAM-1 vs intimal thickening, over time. (E) Quantification of Perl's + DAB, Ly6G, and ORO signal in the intima of mouse carotids over time. Each point represents one mouse. \* $P < 0.05$ , \*\* $P < 0.01$ . Student's *t*-test. (F) Scanning electron microscopy and flow orientation in mouse left common carotid artery subjected to flow perturbation for 3 days. Luminal surface upstream of the cuff (1), within the stenotic site (2), or downstream the cuff (3, 4, and 5). Scale bar: 10  $\mu$ m.

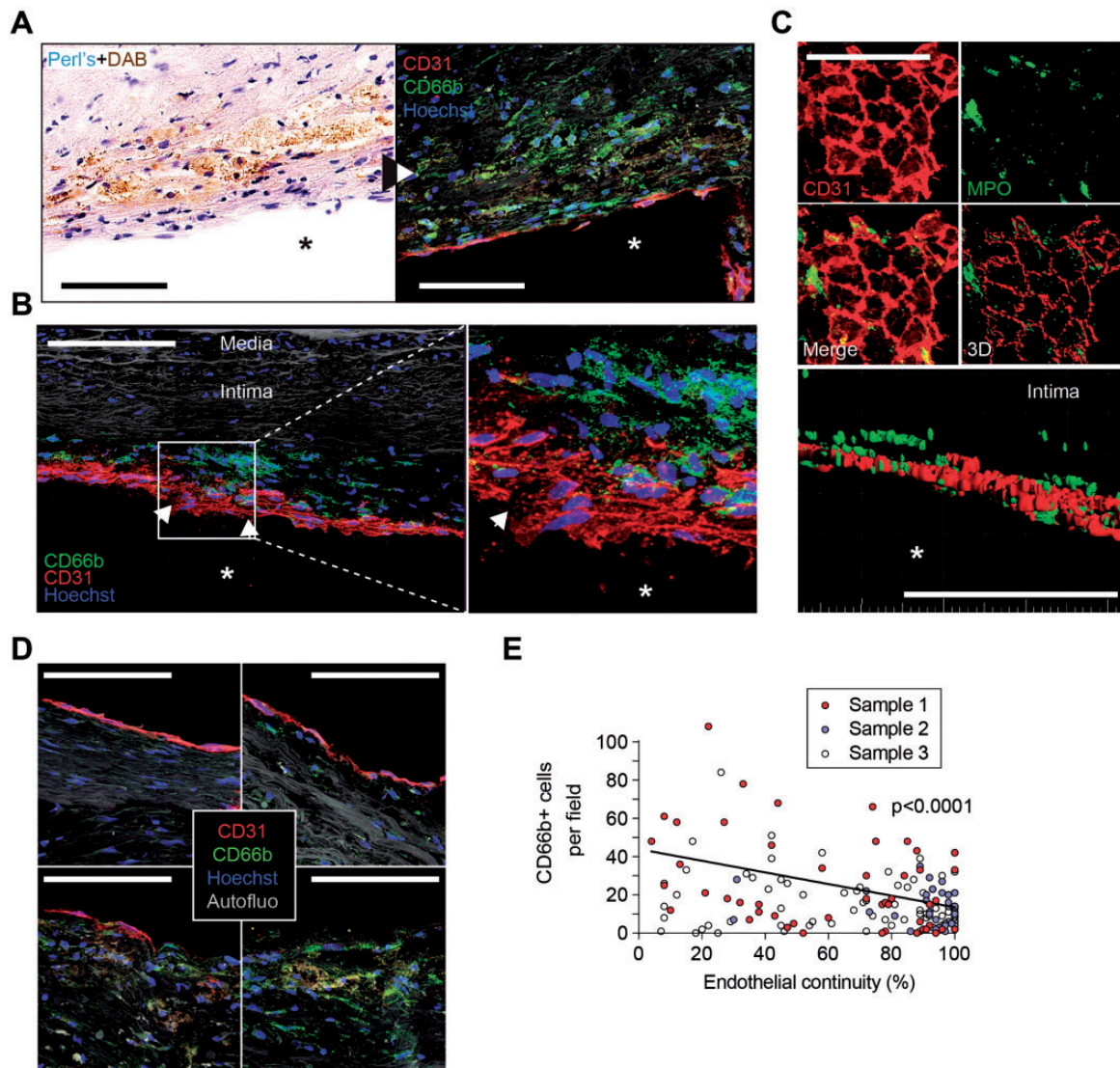


**Figure 4** Intimal breaches, iron deposits, and local granulocyte recruitment. (A) Serial sections of a longitudinally sectioned coronary artery sample showing concomitant iron staining (Perl's + diaminobenzidine) and CD66b<sup>+</sup> granulocytes in superficial intima. Scale bar: 100 µm (B) Immunofluorescent staining for endothelial cells (CD31), granulocytes (CD66b), and nuclei (Hoechst) showing putative intimal breach (arrows) in coronary artery. Scale bar: 200 µm. (C) En face immunofluorescent visualization of early fatty streak in a whole mount preparation of a coronary artery showing intimal accumulation of myeloperoxidase positive granulocytes near luminal endothelial cells (CD31). Scale bar: 100 µm. (D) Negative correlation between local CD66b<sup>+</sup> cell count and endothelial continuity quantified from the CD31 immunofluorescent staining of longitudinally-sectioned coronary arteries from three donors. Scale bar: 100 µm. Numerical correlation is shown in (E). Pearson correlation coefficient was used.

## Discussion

The mechanisms responsible for the ignition of the atherogenic inflammatory response remain poorly understood. This study established a mechanistic link between haemodynamic, intimal breaches, inflammation, and atherogenesis (*Take home figure*). Intimal breaches associated with leucocyte infiltration could be documented in a large number of the human coronary artery samples investigated *ex vivo* and *in vivo* experiments in atherosclerosis prone mice, subjected to haemodynamic stress exacerbation, suggest that focal, mechanical intimal injuries can ignite the inflammatory process underlying atherogenesis.

The presence of intimal breaches in human coronary artery samples localized at sites of perturbed vectors of the direction of flow. These defects were associated with the presence of numerous blood cells, mainly erythrocytes and leucocytes, an observation replicated in the mouse carotids subjected to disturbed flow model. Our findings agree with the pioneering observations made by the group of M.J. Davies, showing that the luminal endothelium in coronary arteries exhibit areas of endothelial layer discontinuity, in the absence of luminal thrombi.<sup>4</sup> Our observations also echo the Virchow's triad theory postulated in the 19th century, and emphasized by Ross in the

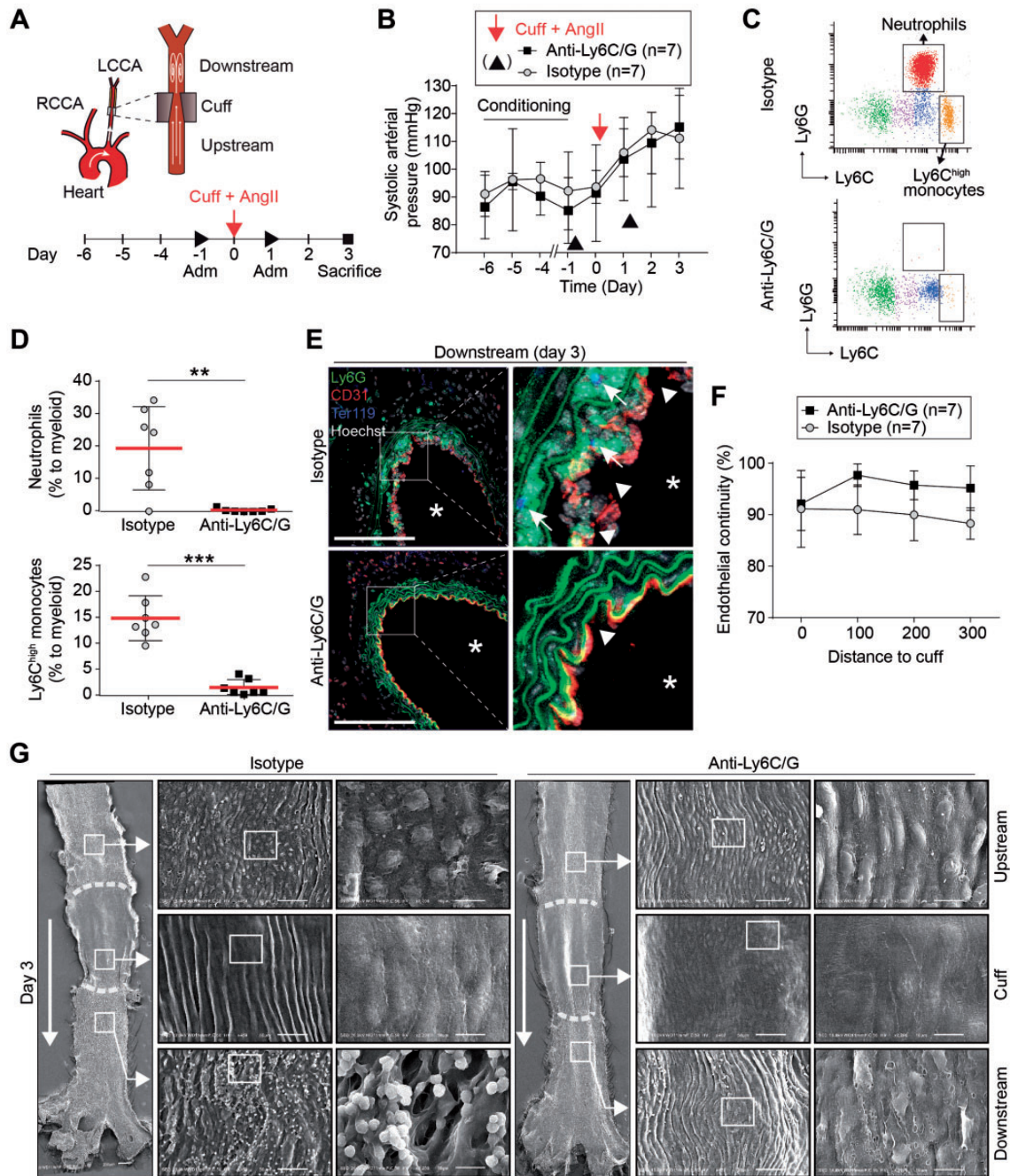
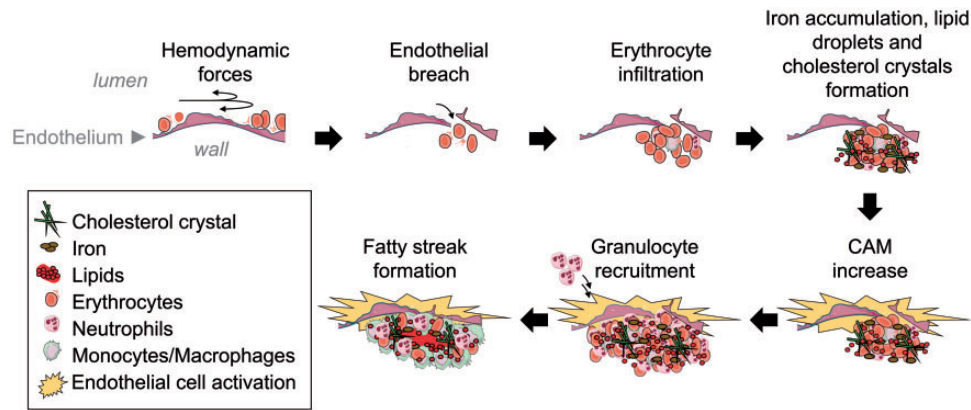


**Figure 5** Impact of neutropenia on flow-induced intimal defects *in vivo*. (A) Flow perturbation was generated in the left common carotid artery of *apoe*<sup>-/-</sup> mice rendered hypertensive after the subcutaneous implantation of an Ang II osmotic pump (delivering 1 mg Ang II/kg/day). LCCA, left common carotid artery; RCCA, right common carotid artery. Anti-Ly6C/G (clone GR1) or an isotype antibody was administered i.p. twice, at Day -1 and Day 1. Mice were euthanized at Day 3. (B) Systolic arterial pressure was monitored in conscious mice everyday between Day -6 and Day -4 (conditioning) and between Day -1 and Day 3 (experience). (C) Blood analysis by cytometry of mice treated with an isotype or the anti-Ly6C/G antibody: gated CD11b<sup>+</sup>CD45<sup>+</sup> cell population is shown on a Ly6G vs. Ly6C scatter plot. Ly6C<sup>+</sup>Ly6G<sup>+</sup> neutrophil (Ly6C<sup>+</sup>Ly6G<sup>+</sup>) and Ly6C<sup>high</sup>Ly6G<sup>-</sup> monocyte populations are highlighted by insets in both groups. Quantification is shown in (D) for Ly6G<sup>+</sup> neutrophils and Ly6C<sup>high</sup> monocytes. Each point represents one mouse. \*\**P* < 0.01, \*\*\**P* < 0.001. Mann-Whitney *U* test. (E) Immunofluorescent staining of downstream carotid cross sections from both groups at Day 3 for neutrophils (Ly6G, green), endothelial cells (CD31, red), erythrocytes (Ter119, blue), and nuclei (Hoechst, white). Stars indicate the carotid lumen; arrows point at erythrocytes; arrowheads show intimal breaches. Scale bar: 100 μm. (F) CD31/morphometry-based quantification of endothelial continuity in the carotid lumen of both groups. The serial segments studied are located between 0 and 300 μm of the cuff. (G) En face scanning electron microscopy showing the luminal surface of the carotids from both groups. Arrows show flow orientation. Dashed lines show the position of the cuff. Insets focus on upstream, cuff or downstream segments. Scale bar: 10 μm.



**Take home figure** Haemodynamic forces induce the formation of endothelial breaches, causing the entry of erythrocyte in the subintimal space. Cholesterol structures, derived from the erythrocytes' membranes, trigger the expression of cell adhesion molecules (CAM) by the overlying endothelial cells, driving an inflammatory process via the recruitment of granulocytes resulting in the formation of fatty streaks at the site of intimal wounding.

late 70's,<sup>8</sup> designating flow and endothelial injury as a *primum movens* of atherosclerosis. The emergence of concepts involving the penetration of lipoproteins as a source of cholesterol and qualitative endothelial dysfunction triggered specifically by lipoprotein oxidation eclipsed these pivotal notions, later on. The observations made in the present work revisit the role of intimal breaches as one early contributor to lesion initiation in arterial regions that experience flow disturbances. The use of modern technology redefined the central role played by these haemodynamically-related microscopic lesions in the process of atherogenesis.

Neutrophils are the most abundant formed elements within human blood after RBCs and platelets and are the first leucocytes recruited to sites of acute injury where they play key roles in the acute inflammatory processes that precede wound healing. Acute neutrophilic response must however be followed by a resolution phase to restore tissue homeostasis, because the persistence of neutrophils can also contribute to aggravate tissue injury as they release toxic agents ranging from proteases to oxygen species. The involvement of neutrophils in atherogenesis has largely been debated in the past but is nowadays widely recognized.<sup>9,10</sup> We found numerous neutrophils accumulating at the site of intimal breaches, in both human and mouse arteries, and the results of the depletion experiments suggests that the collateral damage caused by the infiltrated neutrophils plays an essential role in the transformation of the subintimal haemorrhages in fatty streaks, at sites of disturbed arterial haemodynamic. The presence of ceroids and cholesterol crystal at the site of erythrocyte accumulation, and the dynamic expression of VCAM-1 following experimental arterial wounding in our study, can provide a mechanistic link between the occurrence of mechanically induced injury of the arterial intima and the development of an atherogenic local inflammatory process. The lipid cargo deriving from the membranes of the erythrocytes trapped in the subintimal space can generate both ceroids and cholesterol crystals, which can activate the inflammasome and induce the expression of cell adhesion molecules by the overlying ECs,<sup>11</sup> explaining the dramatic infiltration of neutrophils at the sites of the intimal breaches.

This study used the presence of iron as a biomarker of impaired endothelial integrity and erythrocyte accumulation, but we did not aim to investigate the causal role of iron in atherogenesis. Indeed, the redox-active ferrous iron ( $\text{Fe}^{2+}$ ) from erythrocyte heme prosthetic groups can contribute to catalyse local oxidative activities, in part due to hydroxyl radicals derived through Fenton chemistry.<sup>12</sup> In addition, molecules involved in the metabolism of iron link to atherogenesis: ferritin gene expression occurs in atherosclerotic arterial segments<sup>13</sup> and genome wide association studies show that hepcidin and iron metabolic molecules are associated with atherosclerosis. High throughput screening recently identified heme-oxygenase-1 and biliverdin, two actors of heme catabolism, as markers associating with the severity of atherosclerosis.<sup>14</sup> Further studies are warranted, in particular to assess whether the management of the heme-derived iron by early recruited neutrophils or more broadly by the resident leucocytes, can amplify the impact of iron on the biology of the vessel wall.

Based on clinical and experimental observations, the current paradigm links low (flow reduction) or oscillatory shear stress (recirculation and eddies) with atherosclerosis.<sup>15–17</sup> However, the respective role of these different forms of haemodynamic stresses on atherogenesis remains ill defined. While low shear stress associates with the emergence of lesions with vulnerable characteristics, oscillatory shear stress characterized by recirculation correlates with the formation of more stable plaques with less inflammation.<sup>18</sup> Yet, the mechanisms that initiate these distinct forms of remodelling remain unknown. Novel *in vivo* experimental approaches, such as the one used here, mimicking both low and oscillatory condition *in vivo* may permit distinguishing the differential effects of shear and vector altered patterns in atherogenesis, possibly leading to different types of atherosclerotic lesions.<sup>18,19</sup> Endothelial breaches in areas of flow disturbance may constitute a haemodynamic trigger of atheroma formation, possibly also impacting the morphology of plaques at specific sites of arterial haemodynamic stress. In the context of generalized lipid lowering strategies which decrease the proportion of patients with acute coronary syndromes (ACS) caused by thin-capped 'vulnerable' plaques,

resulting in a relative increase in the proportion of ACS caused by more fibrous plaques with erosion and calcifications as new culprit mechanisms,<sup>20</sup> studies that link different biological causes to plaque morphology hold great interest.

## Study limitations

Human studies were conducted *ex vivo*. In order to limit experimental artefacts, the presence of intimal tears was evaluated on coronary samples dissected from explanted hearts harvested on live patients undergoing heart transplantation and devoid of macroscopic atherosclerotic lesions. Samples were immediately washed and carefully processed, on ice, within the next hours. The presence of erythrocytes in and around breaching areas indicated that the blood had penetrated before the surgical procedure.

The study of flow perturbation in *in vivo* experimental settings provides a useful investigative tool, although we recognize the complexity of the involved effectors, combining the mechanic flow perturbation induced by the application of the cuff<sup>5</sup> with the genetically determined hypercholesterolaemia and the pleiotropic effects of angiotensin II perfusion, which include but are not restricted to the induction of high blood pressure.<sup>21,22</sup> Alternative models of hypertension (e.g. L-NAME, adrenaline) would likely set apart the possible biases brought by the multiple biological effects of angiotensin II. Another limitation of such model resides in the time considerations: the occurrence of artificial endothelial breaches and the ensuing atherogenesis occur in a short time lag in mice, whereas atherosclerosis evolves over decades in humans, possibly biasing the interpretation of mouse experiments in regard of human pathology.

Definitively, the study of the link between mechanically induced endothelial breaches, inflammation, and atheroma onset would benefit from the availability of a multimodal, non-invasive imaging strategy, including for instance the use of magnetic resonance imaging, allowing serial observation in humans.

## Supplementary material

Supplementary material is available at *European Heart Journal* online.

## Acknowledgements

We thank Sigolène Meilhac (Imagine Pasteur, Necker) for her help with HREM. We are grateful to Nadège Anizan, Rachida Aid, and Clément Journé (Fédération de Recherche en Imagerie Multimodalités, FRIM), for providing help with CT scan imaging and arterial pressure measurements.

## Funding

This work was supported by the Institut National de la Santé et de la Recherche Médicale (INSERM), Paris Denis Diderot University, the RHU STOP-AS [#ANR-16-RHUS-0003] from the French National Research Agency (ANR) as part of the 'Investissements d'Avenir' program, and a grant from the Fondation de France [N° Engt: 2013 00038582]. G.F. was supported by the Lefoulon-Delalande foundation (Paris, France), the European Union PRESTIGE programme [2017-1-0032], and the RHU iVASC [#ANR-16-RHUS-00010].

**Conflict of interest:** none declared.

## References

- Delbosc S, Bayles RG, Laschet J, Ollivier V, Ho-Tin-Noe B, Touat Z, Deschildre C, Morvan M, Louedec L, Gouya L, Guedj K, Nicoletti A, Michel JB. Erythrocyte efferocytosis by the arterial wall promotes oxidation in early-stage atheroma in humans. *Front Cardiovasc Med* 2017;**4**:1–15.
- Gimbrone MA Jr, Garcia CG. Endothelial cell dysfunction and the pathobiology of atherosclerosis. *Circ Res* 2016;**118**:620–636.
- Davies PF, Remuzzi A, Gordon EJ, Dewey CF Jr, Gimbrone MA Jr. Turbulent fluid shear stress induces vascular endothelial cell turnover *in vitro*. *Proc Natl Acad Sci USA* 1986;**83**:2114–2117.
- Davies MJ, Woolf N, Rowles PM, Pepper J. Morphology of the endothelium over atherosclerotic plaques in human coronary arteries. *Br Heart J* 1988;**60**:459–464.
- Franck G, Mawson T, Sausen G, Salinas M, Masson GS, Cole A, Beltrami-Moreira M, Chatzizisis Y, Quillard T, Tesmenitsky Y, Shvartz E, Sukhova GK, Swirski FK, Nahrendorf M, Aikawa E, Croce KJ, Libby P. Flow perturbation mediates neutrophil recruitment and potentiates endothelial injury via TLR2 in mice: implications for superficial erosion. *Circ Res* 2017;**121**:31–42.
- Roschztzardt H, Conejero G, Curie C, Mari S. Identification of the endodermal vacuole as the iron storage compartment in the Arabidopsis embryo. *Plant Physiol* 2009;**151**:1329–1338.
- Caro CG, Doorly DJ, Tamawski M, Scott KT, Long Q, Dumoulin CL. Non-planar curvature and branching of arteries and non-planar-type flow. *Proc R Soc Lond A* 1996;**452**:185–197.
- Ross R, Glomset JA. The pathogenesis of atherosclerosis (first of two parts). *N Engl J Med* 1976;**295**:369–377.
- van Leeuwen M, Gijbels MJ, Duijvestijn A, Smook M, van de Gaar MJ, Heeringa P, de Winther MP, Tervaert JW. Accumulation of myeloperoxidase-positive neutrophils in atherosclerotic lesions in LDLR<sup>-/-</sup> mice. *Arterioscler Thromb Vasc Biol* 2008;**28**:84–89.
- Soehnlein O. Multiple roles for neutrophils in atherosclerosis. *Circ Res* 2012;**110**:875–888.
- Duewell P, Kono H, Rayner KJ, Sirois CM, Vladimer G, Bauernfeind FG, Abela GS, Franchi L, Nunez G, Schnurr M, Espevik T, Lien E, Fitzgerald KA, Rock KL, Moore KJ, Wright SD, Hornung V, Latz E. NLRP3 inflammasomes are required for atherogenesis and activated by cholesterol crystals. *Nature* 2010;**464**:1357–1361.
- Formanowicz D, Radom M, Rybarczyk A, Formanowicz P. The role of Fenton reaction in ROS-induced toxicity underlying atherosclerosis—modeled and analyzed using a Petri net-based approach. *Biosystems* 2018;**165**:71–87.
- Pang JH, Jiang MJ, Chen YL, Wang FW, Wang DL, Chu SH, Chau LY. Increased ferritin gene expression in atherosclerotic lesions. *J Clin Invest* 1996;**97**:2204–2212.
- Matic LP, Iglesias MJ, Vesterlund M, Lengquist M, Hong MG, Saieed S, Sanchez-Rivera L, Berg M, Razuvaev A, Kronqvist M, Lund K, Caidahl K, Gillgren P, Pontén F, Uhlén M, Schwenk JM, K HG, Paulsson-Berne G, Fagman E, Roy J, Hultgren R, Bergström G, Lehtiö J, Odeberg J, Hedin U. Novel multiomics profiling of human carotid atherosclerotic plaques and plasma reveals biliverdin reductase B as a marker of intraplaque hemorrhage. *JACC Basic Transl Sci* 2018;**3**:464–480.
- Ku DN, Giddens DP, Zarins CK, Glagov S. Pulsatile flow and atherosclerosis in the human carotid bifurcation. Positive correlation between plaque location and low oscillating shear stress. *Arteriosclerosis* 1985;**5**:293–302.
- Pedersen EM, Oyre S, Agerbæk M, Kristensen IB, Ringgaard S, Boesiger P, Paaske WP. Distribution of early atherosclerotic lesions in the human abdominal aorta correlates with wall shear stresses measured *in vivo*. *Eur J Vasc Endovasc Surg* 1999;**18**:328–333.
- Stone PH, Coskun AU, Kinlay S, Clark ME, Sonka M, Wahle A, Ilegbusi OJ, Yeghiazarians Y, Popma JJ, Orav J, Kuntz RE, Feldman CL. Effect of endothelial shear stress on the progression of coronary artery disease, vascular remodeling, and in-stent restenosis in humans: *in vivo* 6-month follow-up study. *Circulation* 2003;**108**:438–444.
- Cheng C, Tempel D, van Haperen R, van der Baan A, Grosveld F, Daemen MJ, Krams R, de Crom R. Atherosclerotic lesion size and vulnerability are determined by patterns of fluid shear stress. *Circulation* 2006;**113**:2744–2753.
- van Bochove GS, Straathof R, Krams R, Nicolay K, Strijkers GJ. MRI-determined carotid artery flow velocities and wall shear stress in a mouse model of vulnerable and stable atherosclerotic plaque. *MAGMA* 2010;**23**:77–84.
- Libby P, Pasterkamp G. Requiem for the 'vulnerable plaque'. *Eur Heart J* 2015;**36**:2984–2987.
- Pueyo ME, Gonzalez W, Nicoletti A, Savoie F, Arnal JF, Michel JB. Angiotensin II stimulates endothelial vascular cell adhesion molecule-1 via nuclear factor- $\kappa$ B activation induced by intracellular oxidative stress. *Arterioscler Thromb Vasc Biol* 2000;**20**:645–651.
- Piqueras L, Kubes P, Alvarez A, O'Connor E, Issekutz AC, Esplugues JV, Sanz M-J. Angiotensin II induces leukocyte-endothelial cell interactions *in vivo* via AT(1) and AT(2) receptor-mediated P-selectin upregulation. *Circulation* 2000;**102**:2118–2123.